tvst

Article

Ability of Macular Inner Retinal Layer Thickness Asymmetry Evaluated by Optical Coherence Tomography to Detect Preperimetric Glaucoma

Daisuke Takemoto[1], Tomomi Higashide[1], Shinji Ohkubo[1], Sachiko Udagawa[1], and Kazuhisa Sugiyama[1]

[1] Department of Ophthalmology, Kanazawa University Graduate School of Medical Science, Kanazawa, Japan

Correspondence: Daisuke Takemoto, Department of Ophthalmology, Kanazawa University Graduate School of Medical Science, 13-1 Takara-machi, Kanazawa-shi, Ishikawa-ken 920-8641, Japan. e-mail: takemoto0921@med.kanazawa-u.ac.jp

Received: December 1, 2019
Accepted: January 9, 2020
Published: April 15, 2020

Keywords: asymmetry; preperimetric glaucoma; optical coherence tomography; macular ganglion cell layer/inner plexiform layer thickness; ganglion cell complex thickness

Citation: Takemoto D, Higashide T, Ohkubo S, Udagawa S, Sugiyama K. Ability of macular inner retinal layer thickness asymmetry evaluated by optical coherence tomography to detect preperimetric glaucoma. Trans Vis Sci Tech. 2020;9(5):8, https://doi.org/10.1167/tvst.9.5.8

Purpose: We assessed the ability to detect preperimetric glaucoma (PPG) based on asymmetry in the thickness of the macular inner retinal layers measured by spectral-domain optical coherence tomography.

Methods: We studied 45 normal eyes and 50 PPG eyes retrospectively. Three-dimensional optical coherence tomography macular area scans were used to obtain the thickness of the retinal nerve fiber layer (RNFL), ganglion cell layer/inner plexiform layer (GCL/IPL), and ganglion cell complex (GCC). We calculated the thickness differences between the upper and lower macular hemispheres for the corresponding superpixels, then evaluated the mean absolute value of the thickness differences and the number of superpixels in which the thickness difference was greater than X µm, where X is an integer number from 1 to 10. Areas under the receiver operating characteristic curves (AUCs) for their PPG diagnostic performances were compared to the average thickness measurements of the total and hemiretinal sectors. X was determined at the maximum AUC value.

Results: The AUC for the mean absolute value of the difference in GCL/IPL thickness (0.923) was higher than the difference in RNFL and GCC thickness (0.710 and 0.905, respectively). The AUC for the number of superpixels in which the GCL/IPL thickness difference was greater than 8 µm ($X = 8$) was 0.914. The ability to diagnose PPG using these GCL/IPL parameters was statistically higher than for total or superior and inferior hemiretinal GCL/IPL thicknesses.

Conclusions: Asymmetry in the thickness of the GCL/IPL shows good PPG diagnostic performance.

Translational Relevance: This approach would be useful in the early detection of glaucoma.

Introduction

Glaucoma is characterized by the progressive loss of retinal ganglion cells caused by damage to their axons at the optic nerve disc.[1] Exploitation and technological advancement of optical coherence tomography (OCT) has enabled the quantitative assessment of the inner retinal layers containing the retinal ganglion cells by measuring the thickness of the inner retinal layers. Using spectral domain optical coherence tomography (SD-OCT), it has been shown that the thickness of the inner retinal layer is reduced during the early stages of glaucoma.[2,3]

Currently, in the clinical care of glaucoma patients, the thickness parameters of the inner retinal layer (such as the average thickness of the macular area) are often analyzed and assessed by an ophthalmologist, although early-stage preperimetric glaucoma (PPG) can often be missed. However, this type of analysis could be used for detecting early-stage PPG by evaluating the asymmetry in the thickness of the inner retinal layers between the

upper and lower segments of the macula. It is conceivable that this method may be suitable for detecting early-stage PPG, because the loss of disc rim tissue and retinal nerve fiber layer (RNFL) defects are often more severe on either the upper or the lower hemispheres during the early glaucomatous stages.[4,5]

In normal eyes, the retinal layers seem to be fairly symmetric in terms of the mean thickness in the central parafoveal region between the upper and lower segments as determined by SD-OCT.[6] Asymmetrical differences in the thickness of the inner retinal layer between the upper and lower segments of the macula in PPG eyes were initially investigated using SD-OCT in 2011.[7] Since then, several studies have revealed that asymmetry in the thickness of the retinal layers tends to offer better diagnostic performance than assessment of other thickness parameters,[8–14] and asymmetry in the thickness of the ganglion cell layer (GCL)/inner plexiform layer (IPL) tends to offer better diagnostic performance than in the RNFL layer in glaucomatous or PPG eyes.[15] However, the degree of difference between the values of the upper and lower segments of the macular inner retinal layers that defines abnormal conditions in the clinical diagnosis of PPG remains to be determined.

The purpose of the present study was to evaluate asymmetry in the thickness of the inner retinal layer in both PPG eyes and normal eyes and to evaluate its diagnostic ability for detecting PPG in comparison with conventional methods. In addition, we also sought to establish clear criteria for defining asymmetry in the inner retinal layers.

Materials and Methods

Subjects

All of the study participants, including PPG patients and normal subjects, were examined at the Department of Ophthalmology at Kanazawa University Hospital between November 2010 and September 2018. We reviewed the electronic medical records of these subjects in this observational cross-sectional study.

PPG was defined as the following: (1) the existence of characteristic thinning of the optic disc rim, increased cup-to-disc ratio, and notches (glaucomatous optic neuropathy [GON]) with or without RNFL defects; (2) reliable visual field results showing no glaucomatous visual field defects during the course of observation; (3) the presence of a normal open angle; and (4) no ocular or systemic disorders that could cause the visual field defects. GON was determined based on the agreement of three independent blinded glaucoma specialists using fundus photographs including red-free photographs (nonmyd WX3D; Kowa, Inc., Tokyo, Japan). Visual field defects were defined based on these criteria[16]: (1) three or more contiguous points with probabilities of $<5\%$ of not crossing the horizontal meridian line on the pattern deviation map including at least one point with a probability of $<1\%$; (2) a pattern standard deviation outside 95% of normal limits; or (3) an abnormal result on the glaucoma hemifield test as confirmed by reliable examinations (fixation losses $< 20\%$, false positives or negatives $< 15\%$) by standard automated perimetry (Humphrey Visual Field Analyzer II; Swedish Interactive Threshold Algorithm standard 30-2 or 24-2; Carl Zeiss Meditec, Inc., Dublin, CA, USA). Visual field testing, fundus photography, and SD-OCT measurements were performed within a period of 3 months.

The inclusion criteria included (1) best-corrected visual acuity of 0.5 or more, (2) spherical equivalent refractive error between –6 D and 3 D, and (3) age of $\geq$20 years. The exclusion criteria included (1) ocular infection, inflammatory disease, or corneal ulcer that occurred $\leq$1 month before the start of the trial; (2) cataract, retinal disorders, or other disorders that may affect the visual field; (3) history of ocular surgery or laser treatment; and (4) optic nerve degeneration other than glaucoma.

This study was approved by the Institutional Review Board of Kanazawa University, and the study was conducted in full accord with the tenets of the Declaration of Helsinki. Written informed consent was obtained from all subjects after the study protocol was fully explained.

OCT Measurements

Three-dimensional OCT scans (3D OCT-2000 version 8.1x, Topcon, Tokyo, Japan) were acquired from each eye. Scan areas were 7 $\times$ 7 mm centered on the fovea at a scan density of 512 (vertical) $\times$ 128 (horizontal). The thicknesses of the macular RNFL, GCL/IPL, and ganglion cell complex (GCC) were obtained within a 6 $\times$ 6-mm macular area divided into 10 $\times$ 10 grids (i.e., 100 superpixels). The average total thickness and the average superior and inferior hemiretinal thicknesses of the RNFL, GCL/IPL, and GCC were calculated and exported using software provided by Topcon. Internal software also generated a significance map consisting of deviation plots by color-coding the 10 $\times$ 10 grids with no color (within the 95% normal limit), yellow (outside of the 95% normal limit), or red (outside the 99% normal limit).

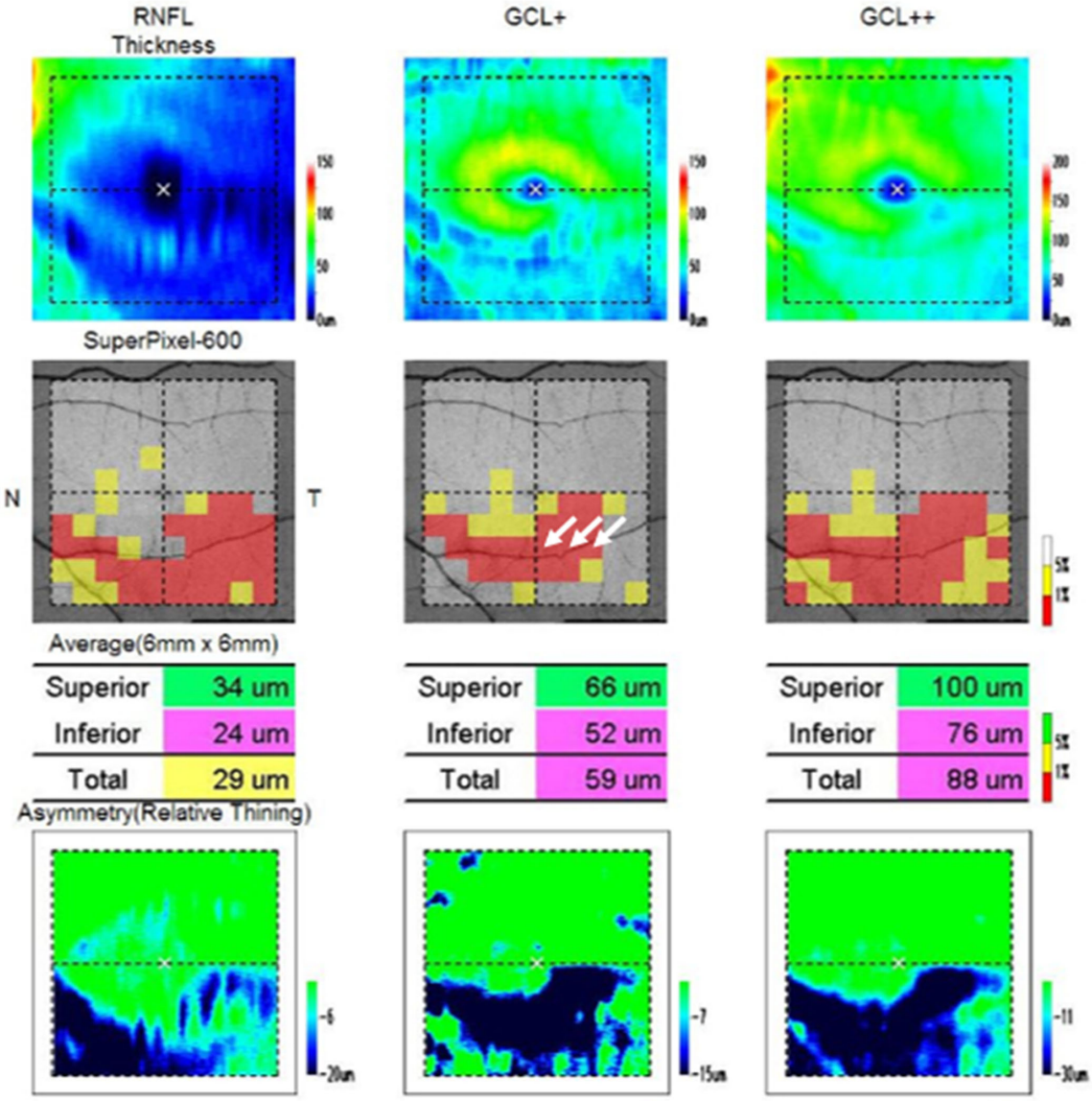

Figure 1. A printout of the macular three-dimensional scan analysis. The viewer shows RNFL thickness, GCL/IPL thickness (GCL+), and GCC thickness (GCL++), starting from the left. In the second line, it shows the significance map consisting of deviation plots by color-coding 10 × 10 grids as clear color (within the 95% normal limit), yellow (outside of the 95% normal limit), or red (outside of the 99% normal limit). Arrows indicate that cluster criteria were fulfilled. The third line shows the average superior and inferior hemiretinal thicknesses and the average total thickness of the RNFL, GCL/IPL, and GCC.

In terms of the GCL/IPL, we adopted the "cluster criteria" concept for the glaucoma criterion by three-dimensional OCT. The cluster criteria were devised by Kanamori and associates[17] as follows: If an eye shows at least three contiguous grids displayed in red for the GCL/IPL measurements of the same hemiretina, the eye is considered to be abnormal (Fig. 1).

Images with a quality factor > 45 and that were first obtained after a diagnosis of PPG were used for analyses. Images including a cycloduction or cyclotorsion as judged using B-scan images were excluded.

Statistical Analysis

All statistical analyses were performed using JMP 12.2 software (SAS Institute Japan, Tokyo, Japan). A Mann–Whitney *U* test was used to compare patient characteristic data (excluding for sex ratio) between normal and PPG eyes. Fisher's exact probability test was used to compare the sex ratio between the two groups.

To evaluate macular asymmetry, we calculated the thickness differences between the upper and lower

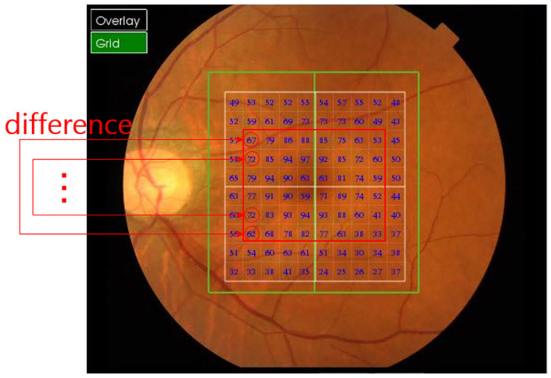

Figure 2. We calculated the thickness differences between the upper and lower macula halves of the subject eyes for each of the corresponding superpixels in 6 × 8 grids centered on the foveal pit (excluding the outer zone of the posterior part to avoid the influence of the large retinal vessels) for the RNFL, GCL/IPL, and GCC.

macular hemispheres of the subject's eyes for each of the corresponding superpixels in 6 × 8 grids centered on the foveal pit (excluding the outer zone of the posterior part to avoid the influence of the large retinal vessels) for the RNFL, GCL/IPL, and GCC (Fig. 2). We evaluated the mean absolute value of the thickness differences and the number of superpixels in which the thickness difference was $\geq X$ µm, where X is an integer number from 1 to 10. These two parameters were termed the asymmetry parameters. We calculated the area under the receiver operating characteristics (ROC) curves (the area under the curve [AUC] values) of the asymmetry parameters to evaluate their PPG diagnostic abilities. X was determined at the maximum AUC value. We then made comparisons of the AUC values between the asymmetry parameters and the average total or superior and inferior hemiretinal thicknesses, according to the methods of DeLong and associates.[18] In terms of GCL/IPL thickness, the sensitivity and specificity of the asymmetry parameters for PPG detection were calculated according to the optimal cutoff point, which was set as the maximum of the Youden index: max(sensitivity + specificity – 1). The sensitivity and specificity of the asymmetry parameters were compared with those of the cluster criteria using the McNemar test. $P < 0.05$ was considered to be statistically significant. Values are stated as the mean ± standard deviation. The data ranges were recorded as the mean ± standard deviation unless otherwise noted.

Results

We studied 45 normal eyes (45 subjects) and 50 PPG eyes (42 PPG patients). The characteristics of the patients in each group are shown in Table 1. There were no statistically significant differences between the PPG and the normal groups in terms of age, sex, visual acuity, spherical equivalent refractive error, intraocular pressure, axial length, or mean deviation. The pattern standard deviation was higher in the PPG group than in the normal group. Average macular RNFL, GCL/IPL, and GCC thickness (total macular area and superior and inferior hemifields) was statistically lower in the PPG group than in the normal group.

Figure 3 shows the ROC curves of the mean absolute value of the thickness differences in the RNFL, GCL/IPL, and GCC. As shown in Table 2, the thickness differences in the GCL/IPL showed the statistically highest AUC value (0.923) compared to the RNFL; there was no significant difference between the GCL/IPL and GCC. Table 3 shows the AUC values for the number of superpixels in which the thickness difference was $\geq X$ µm, where X is a natural number from 1 to 10. X was determined to be 8 at the maximum AUC value for the GCL/IPL or GCC and was determined to be 4 at the maximum AUC value for the RNFL.

Figure 4 shows the ROC curves for the GCL/IPL asymmetry parameters and the average GCL/IPL thickness (for the total macular area and the superior and inferior hemifields). As shown in Table 4, the AUC values for the mean absolute value of the thickness differences in the GCL/IPL and the number of superpixels in which the thickness difference was ≥8 µm were 0.923 and 0.914, respectively. These values were statistically higher than for the GCL/IPL mean thickness in the 6 × 6-mm total area, superior hemifield, and inferior hemifield (these AUC values were 0.769, 0.694, and 0.807, respectively). Figure 5 shows the ROC curves for the GCC asymmetry parameters and average GCC thickness (for the total macular area and the superior and inferior hemifields). As shown in Table 5, the AUC values for the number of superpixels in which the thickness difference of the GCC was ≥8 µm were the highest (0.926), although there was no significant difference between the other parameters (excluding GCC thickness at the superior hemifield). Figure 6 and Table 6 show the ROC curves and the AUC values for the RNFL asymmetry parameters and average RNFL thickness (for the total macular area and the superior and inferior hemifields). There were no primacy of asymmetry parameters over thickness parameters about the RNFL.

As shown in Table 7, for the GCL/IPL, the cluster criteria showed 64% (32/50) sensitivity and 89% (40/45) specificity. The mean absolute value of the asymmetrical differences in thickness in the GCL/IPL showed 90% sensitivity and 85% specificity, and the number of superpixels in which the asymmetrical difference in

Table 1. Patient Characteristics

	PPG Eyes (50 Eyes)	Normal Eyes (45 Eyes)	*P*
Age (y)	60 ± 10	54 ± 17	0.07[a]
Sex, n (%)			0.22[b]
Men	17 (34)	21 (47)	
Women	33 (66)	24 (53)	
Visual acuity, logMAR value	−0.087 ± 0.039	−0.076 ± 0.039	0.15[a]
Refractive value (D)	−1.9 ± 2.4	−2.0 ± 2.3	0.73[a]
Intraocular pressure (mm Hg)	14.8 ± 2.5	14.4 ± 2.2	0.48[a]
Axial length (mm)	24.4 ± 1.7	24.4 ± 1.4	0.90[a]
Mean deviation (dB)	−0.27 ± 1.03	−0.82 ± 1.53	0.24[a]
Pattern standard deviation (dB)	1.70 ± 0.34	1.57 ± 0.81	<0.001[a]
Average thickness in the total 6 × 6 mm area (µm)			
RNFL	31.0 ± 3.9	37.1 ± 4.2	<0.001[a]
GCL/IPL	63.8 ± 5.1	68.8 ± 4.1	<0.001[a]
GCC	94.8 ± 7.7	105.9 ± 6.2	<0.001[a]
Average thickness in the superior hemifield (µm)			
RNFL	31.5 ± 5.0	36.0 ± 4.1	<0.001[a]
GCL/IPL	65.8 ± 5.9	69.6 ± 4.1	0.0011[a]
GCC	97.4 ± 9.7	105.6 ± 6.1	<0.001[a]
Average thickness in the inferior hemifield (µm)			
RNFL	30.5 ± 5.9	38.1 ± 4.7	<0.001[a]
GCL/IPL	61.7 ± 5.9	68.0 ± 4.3	<0.001[a]
GCC	92.2 ± 10.2	106.1 ± 6.6	<0.001[a]

Values represent the mean ± standard deviation.
[a]Mann–Whitney *U* test.
[b]Fisher's exact probability test.

thickness of the GCL/IPL was ≥8 µm showed 86% sensitivity and 87% specificity using the ROC-based cut-off criterion (we set the optimal cutoff values at 4.4 µm and 4.0, respectively). Significant differences were found between the two asymmetry parameters and the cluster criteria ($P < 0.001$ and $P = 0.012$, respectively).

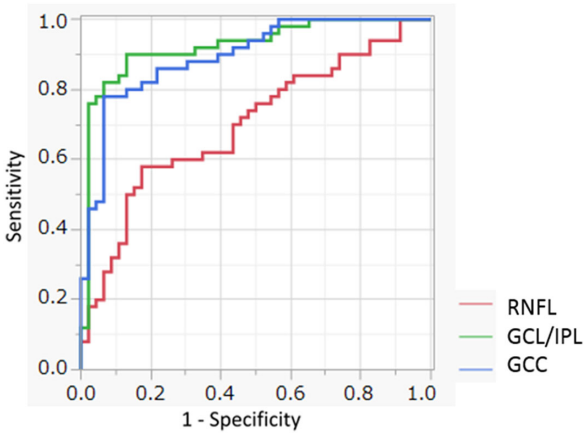

Figure 3. The ROC curves of the mean absolute value of the thickness differences for the RNFL, GCL/IPL, and GCC.

Table 2. AUC Values for the Mean Absolute Value of the Asymmetrical Differences in Thickness of the Macular RNFL, GCL/IPL, and GCC

	AUC	95% Confidence Interval	*P*[a] GCL/IPL	*P*[a] GCC
RNFL	0.710	0.596–0.803	<0.001	<0.001
GCL/IPL	0.923	0.843–0.964	—	0.259
GCC	0.905	0.827–0.951	—	—

[a]Analysis is based on the methods of DeLong and associates.[18]

Figures 7 and 8 show cases where it was confirmed that the appearance of asymmetry in the thickness of the GCL/IPL preceded the appearance of RNFL defects in the fundus photographs or satisfied the cluster criteria. Figure 7 shows the case of a 69-year-old woman. In 2017, the lower side of the RNFL defect appeared in a fundus photograph, and the cluster criteria were fulfilled based on OCT imaging. Dating back to the year 2011, these glaucomatous signs had yet to appear; however, asymmetry in the thickness of the

Table 3. AUC Values for the Number of Superpixels in Which the Differences in Thickness of the Macular RNFL, GCL/IPL, and GCC ≥ *X* µm

	RNFL		GCL/IPL		GCC	
X (µm)	AUC	95% Confidence Interval	AUC	95% Confidence Interval	AUC	95% Confidence Interval
1	0.659	0.543–0.758	0.800	0.692–0.877	0.717	0.603–0.808
2	0.672	0.557–0.770	0.836	0.742–0.900	0.798	0.696–0.872
3	0.710	0.597–0.801	0.859	0.768–0.918	0.799	0.697–0.873
4	0.721[a]	0.609–0.811	0.887	0.801–0.939	0.832	0.738–0.900
5	0.696	0.582–0.789	0.898	0.812–0.947	0.866	0.781–0.922
6	0.692	0.582–0.784	0.902	0.815–0.950	0.896	0.819–0.942
7	0.689	0.574–0.785	0.912	0.833–0.955	0.911	0.840–0.923
8	0.689	0.587–0.776	0.914[a]	0.840–0.962	0.926[a]	0.859–0.962
9	0.663	0.555–0.757	0.900	0.809–0.950	0.924	0.856–0.962
10	0.650	0.546–0.733	0.898	0.804–0.949	0.921	0.844–0.962

[a]AUC maximum values.

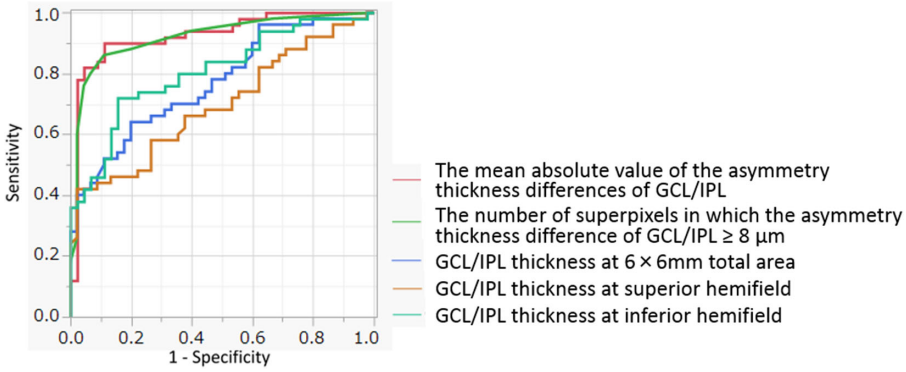

Figure 4. The ROC curves for GCL/IPL asymmetry parameters and averages of GCL/IPL thickness (at the total visual field and the superior and inferior hemifields).

GCL/IPL layer between the upper and lower segments had already been evident. At that date, the values of the two asymmetry parameters (the mean absolute value of the thickness differences in the GCL/IPL and the number of superpixels in which the GCL/IPL thickness difference was ≥8 µm) had exceeded the cutoff limits (5.4 and 7.0, respectively). Figure 8 shows the case of a 68-year-old woman. In 2017, the upper side

Table 4. AUC Values for the Asymmetry Parameters and Thickness Parameters of the GCL/IPL

	AUC	95% Confidence Interval	*P*[a]			
			Number	Total	Superior	Inferior
Mean absolute value of the asymmetrical differences in thickness of the GCL/IPL	0.923	0.843–0.964	0.473	0.002	<0.001	0.008
Number of superpixels in which the asymmetrical difference in thickness of the GCL/IPL was ≥8 µm	0.914	0.834–0.958	—	0.006	<0.001	0.02
GCL/IPL thickness in the total 6 × 6-mm area	0.769	0.663–0.849	—	—	0.006	0.17
GCL/IPL thickness in the superior hemifield	0.694	0.579–0.788	—	—	—	0.02
GCL/IPL thickness in the inferior hemifield	0.807	0.705–0.880	—	—	—	—

[a]Analysis is based on the methods of DeLong and associates.[18]

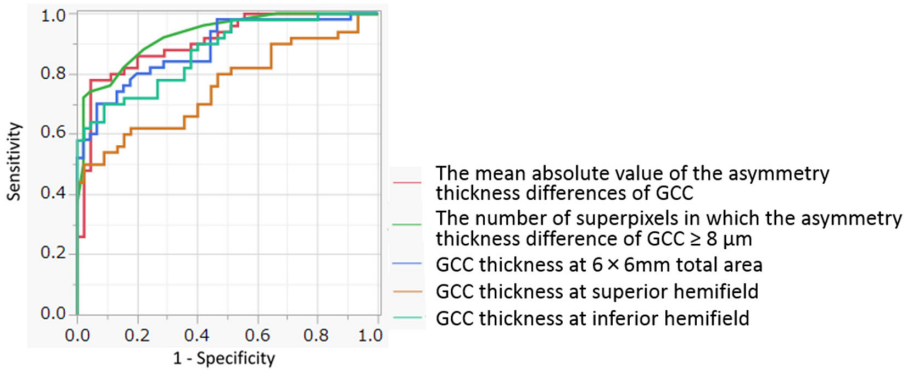

Figure 5. The ROC curves for GCC asymmetry parameters and averages of GCC thickness (at the total visual field and the superior and inferior hemifields).

Table 5. AUC Values for the Asymmetry Parameters and Thickness Parameters of the GCC

	AUC	95% Confidence Interval	*P*[a]			
			Number	Total	Superior	Inferior
Mean absolute values of the asymmetrical differences in thickness of the GCC	0.905	0.827–0.951	0.107	0.610	0.012	0.470
Number of superpixels in which the asymmetrical difference in thickness of the GCC was ≥8 µm	0.926	0.859–0.962	—	0.296	0.003	0.216
GCC thickness in the total 6 × 6-mm area	0.883	0.800–0.935	—	—	<0.001	0.706
GCC thickness in the superior hemifield	0.758	0.648–0.842	—	—	—	0.019
GCC thickness in the inferior hemifield	0.873	0.789–0.927	—	—	—	—

[a] Analysis is based on the methods of DeLong and associates.[18]

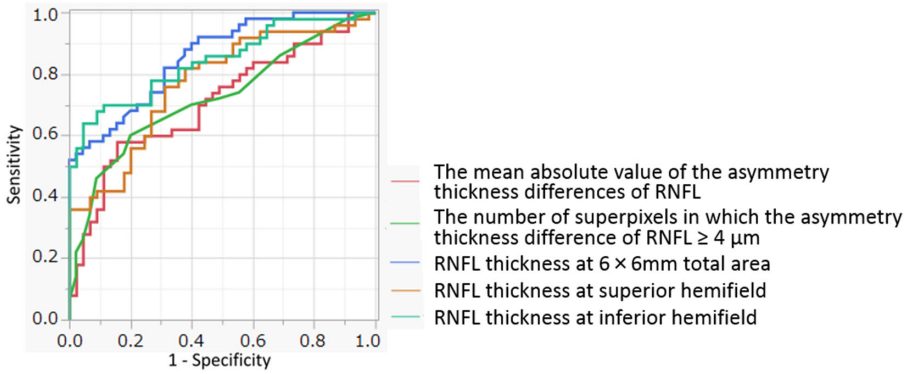

Figure 6. The ROC curves for RNFL asymmetry parameters and averages of RNFL thickness (at the total visual field and the superior and inferior hemifields).

of the RNFL defect appeared in a fundus photograph, and the cluster criteria were fulfilled based on OCT imaging. Dating back to the year 2013, although these glaucomatous signs had yet to appear, asymmetry in the thickness of the GCL/IPL layer between the upper and lower segments had already become evident. At that date, the values of the two asymmetry parameters had exceeded the cutoff limits (6.1 and 7.0, respectively). Going back further to the year 2010, the asymmetry in the thickness of the inner retinal layers between the upper and lower segments had not yet appeared, and the values of the two parameters had not exceeded the cutoff limits (2.8 and 0, respectively).

Table 6. AUC Values for the Asymmetry Parameters and Thickness Parameters of the RNFL

	AUC	95% Confidence Interval	*P*[a]			
			Number	Total	Superior	Inferior
Mean absolute value of the asymmetrical differences in thickness of the RNFL	0.710	0.596–0.803	0.562	0.037	0.405	0.068
Number of superpixels in which the asymmetrical difference in thickness of the RNFL was ≥4 µm	0.721	0.609–0.811	—	0.048	0.478	0.092
RNFL thickness in the total 6 × 6-mm area	0.856	0.768–0.914	—	—	0.011	0.657
RNFL thickness in the superior hemifield	0.772	0.664–0.852	—	—	—	0.178
RNFL thickness in the inferior hemifield	0.844	0.750–0.907	—	—	—	—

[a]Analysis is based on the methods of DeLong and associates.[18]

Table 7. Sensitivity and Specificity of the Cluster Criteria and Asymmetry Parameters of the GCL/IPL

	Sensitivity	Specificity	*P*[a]	
			Cluster Criteria	Mean[b]
Cluster criteria	64.0%	88.9%	—	—
Mean absolute value of the asymmetrical differences in thickness of the GCL/IPL	90.0%	84.8%	<0.001	—
Number of superpixels in which the asymmetrical difference in thickness of the GCL/IPL was ≥8 µm	86.0%	87.0%	0.012	0.71

[a]McNemar test.
[b]Mean is the mean absolute value of the asymmetrical difference in thickness.

Discussion

In the present study, we investigated whether the assessment of asymmetry in the inner retinal layers between the upper and lower segments of the macula would outperform the inner retinal layer thickness parameters for the detection of PPG. Summarizing the results, first, the ability to diagnose PPG using the

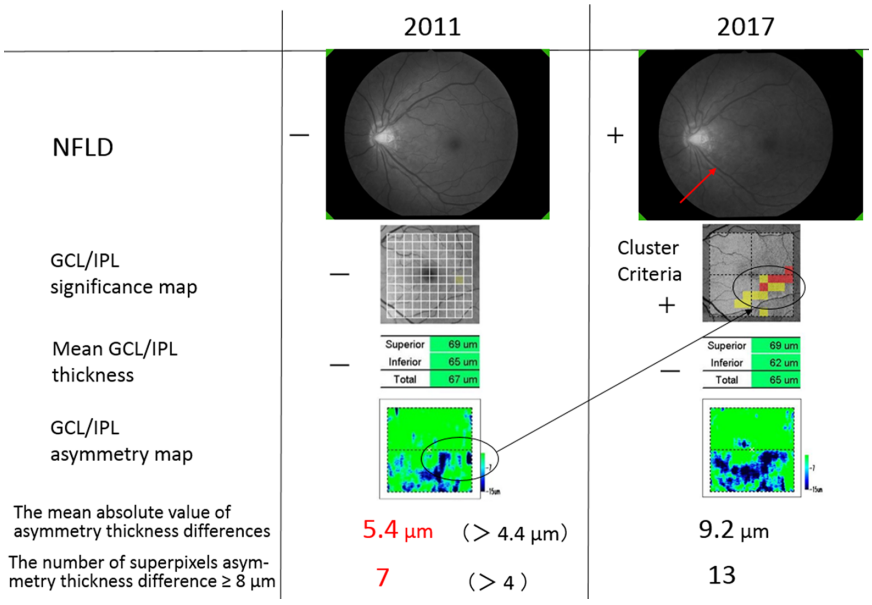

Figure 7. In 2011, any glaucomatous sign by fundus photograph or OCT imaging had not yet appeared in this 69-year-old woman, but asymmetry of thickness of the GCL/IPL between the upper and lower segments had already appeared clearly. Two asymmetry parameters are shown for GCL/IPL.

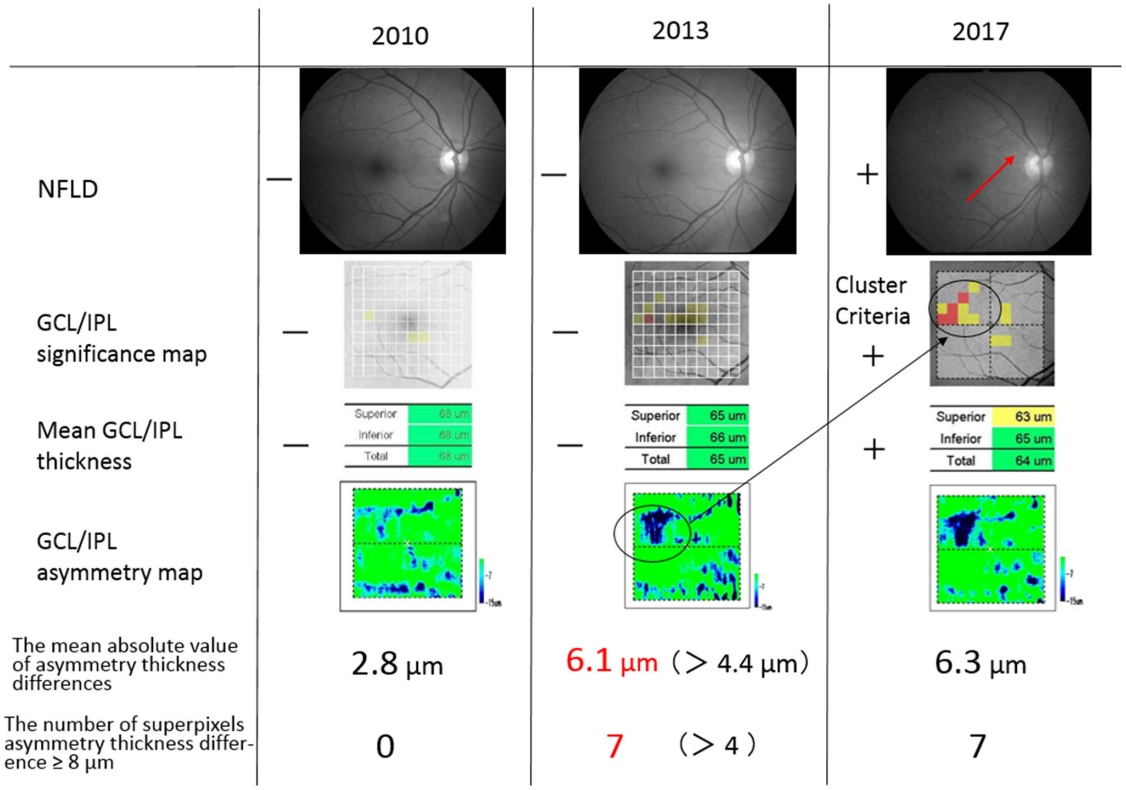

Figure 8. In 2013, any glaucomatous sign by fundus photograph or OCT imaging had not yet appeared in this 68-year-old woman, but asymmetry of thickness of the GCL/IPL between the upper and lower segments had already appeared clearly. Two asymmetry parameters are shown for GCL/IPL.

asymmetry of the GCL/IPL or GCC was higher than for the RNFL. Second, the ability to diagnose PPG using asymmetry parameters was better than using thickness parameters with regard to the GCL/IPL. Third, the ability to diagnose PPG using the asymmetry of the GCL/IPL was higher than using the cluster criteria, an index of glaucomatous change determined using the Topcon 3D OCT-2000.

Yamada and associates[15] determined that diagnosing PPG using asymmetry of the GCL/IPL compared to using thickness parameters was better than for the GCC or RNFL. Moreover, Kim and associates[12] also showed that the ability to diagnosis PPG was higher using the asymmetry of the GCL/IPL than using GCL/IPL thickness parameters. Both of these previous studies were consistent with our present results. In the current study, we identified a PPG diagnostic difference value between the upper and lower segments of the macular inner retinal layers for the first time. Lee and associates[19] suggested 20 μm as the difference value between the upper and lower segments of the GCL/IPL, but their study applied only to glaucomatous eyes, not PPG eyes. We assume that the asymmetry in thickness of the inner retinal layers between the upper and lower segments is more useful for discriminating between normal eyes and PPG eyes than for eyes with progressive glaucoma. This is because the asymmetry in macular retinal thickness can be somewhat unclear during the progressive stage in glaucomatous eyes.

We hypothesized that the appearance of asymmetry in retinal thickness as revealed by OCT is an initial sign of glaucoma onset. In our present study, we encountered several cases that supported this hypothesis. There were five patients (five eyes) in which we captured OCT data prior to the appearance of glaucomatous changes in the fundus. In all five cases, it was confirmed that the appearance of asymmetry in the thickness of the GCL/IPL preceded the appearance of RNFL defects in the fundus photographs or satisfied the cluster criteria. Two of the cases are shown in Figures 7 and 8.

Our study has a few limitations that should be noted. First, the study design was retrospective. Second, we exclusively used the horizontal line passing through the fovea but not through the optic disc center. It is possible that using the strict fovea–disc line as the axis of symmetry might have given more

accurate results; however, Hirasawa and associates[20] reported that correction of ocular rotation had no substantial effect on the reproducibility of the SD-OCT measurements in normal and glaucoma eyes. In addition, it is not clear whether the strict fovea–disc line is a true axis of symmetry. A recent report[21] showed that the horizontal raphe in the temporal macular area was different from the fovea–disc line. Another study[22] reported that the structural temporal raphe was more deviated to the perimetrically normal hemiretinal side than to the functional temporal raphe in eyes with a glaucomatous hemifield defect. A third limitation is that there were only five patients in which we captured OCT data prior to the appearance of glaucomatous changes to the fundus which could be used to demonstrate that the appearance of asymmetry in retinal thickness revealed by OCT is an initial sign of glaucoma onset. We think that a prospective study further evaluating this hypothesis is warranted.

Conclusions

We quantitatively revealed that asymmetry in the thickness of the inner retinal layers (especially the GCL/IPL) shows good diagnostic performance for PPG, and we presented clinical indices and cutoff values for the asymmetry in the inner retinal layers. Furthermore, we hypothesize that the appearance of asymmetry in retinal thickness as revealed by OCT is an initial sign of glaucoma onset, but this hypothesis must be studied in more early-stage PPG subjects. We believe that the asymmetry parameters determined here will be useful as structural markers for early-stage glaucoma.

Acknowledgments

Supported by Japan Society for the Promotion of Science KAKENHI Grant No. 19K18840.

Disclosure: **D. Takemoto**, None; **T. Higashide**, None; **S. Ohkubo**, None; **S. Udagawa**, None; **K. Sugiyama**, None

References

1. Quigley HA, Dunkelberger GR, Green WR. Retinal ganglion cell atrophy correlated with automated perimetry in human eyes with glaucoma. *Am J Ophthalmol*. 1989;107:453–464.
2. Seong M, Sung KR, Choi EH, et al. Macular and peripapillary retinal nerve fiber layer measurements by spectral domain optical coherence tomography in normal-tension glaucoma. *Invest Ophthalmol Vis Sci*. 2010;51:1446–1452.
3. Kotera Y, Hangai M, Hirose F, Mori S, Yoshimura N. Three-dimensional imaging of macular inner structures in glaucoma by using spectral-domain optical coherence tomography. *Invest Ophthalmol Vis Sci*. 2011;52:1412–1421.
4. Quigley HA, Katz J, Derick RJ, Gilbert D, Sommer A. An evaluation of optic disc and nerve fiber layer examinations in monitoring progression of early glaucoma damage. *Ophthalmology*. 1992;99:19–28.
5. Quigley HA, Dunkelberger GR, Green WR. Chronic human glaucoma causing selectively greater loss of large optic nerve fibers. *Ophthalmology*. 1988;95:357–363.
6. Ooto S, Hangai M, Tomidokoro A, et al. Effects of age, sex, and axial length on the three-dimensional profile of normal macular layer structures. *Invest Ophthalmol Vis Sci*. 2011;52:8769–8779.
7. Nakano N, Hangai M, Nakanishi H, et al. Macular ganglion cell layer imaging in preperimetric glaucoma with speckle noise-reduced spectral domain optical coherence tomography. *Ophthalmology*. 2011;118:2414–2426.
8. Um TW, Sung KR, Wollstein G, Yun SC, Na JH, Schuman JS. Asymmetry in hemifield macular thickness as an early indicator of glaucomatous change. *Invest Ophthalmol Vis Sci*. 2012;53:1139–1144.
9. Seo JH, Kim TW, Weinreb RN, Park KH, Kim SH, Kim DM. Detection of localized retinal nerve fiber layer defects with posterior pole asymmetry analysis of spectral domain optical coherence tomography. *Invest Ophthalmol Vis Sci*. 2012;53:4347–4353.
10. Sullivan-Mee M, Ruegg CC, Pensyl D, Halverson K, Qualls C. Diagnostic precision of retinal nerve fiber layer and macular thickness asymmetry parameters for identifying early primary open-angle glaucoma. *Am J Ophthalmol*. 2013;156:567–577.
11. Kawaguchi C, Nakatani Y, Ohkubo S, Higashide T, Kawaguchi I, Sugiyama K. Structural and functional assessment by hemispheric asymmetry testing of the macular region in preperimetric glaucoma. *Jpn J Ophthalmol*. 2014;58:197–204.
12. Kim YK, Yoo BW, Kim HC, Park KH. Automated detection of hemifield difference across horizontal raphe on ganglion cell-inner plexiform layer thickness map. *Ophthalmology*. 2015;122: 2252–2260.

13. Khanal S, Davey PG, Racette L, Thapa M. Intra-eye retinal nerve fiber layer and macular thickness asymmetry measurements for the discrimination of primary open-angle glaucoma and normal tension glaucoma. *J Optometry*. 2016;9:118–125.
14. Sharifipour F, Morales E, Lee JW, et al. Vertical macular asymmetry measures derived from SD-OCT for detection of early glaucoma. *Invest Ophthalmol Vis Sci*. 2017;58:4310–4317.
15. Yamada H, Hangai M, Nakano N, et al. Asymmetry analysis of macular inner retinal layers for glaucoma diagnosis. *Am J Ophthalmol*. 2014;158:1318–1329.
16. Anderson DR, Patella VM. *Automated Static Perimetry*. 2nd ed. St. Louis, MO: Mosby; 1999:121–190.
17. Kanamori A, Naka M, Akashi A, Fujihara M, Yamada Y, Nakamura M. Cluster analyses of grid-pattern display in macular parameters using optical coherence tomography for glaucoma diagnosis. *Invest Ophthalmol Vis Sci*. 2013;54:6401–6408.
18. DeLong ER, DeLong DM, Clarke-Pearson DL. Comparing the areas under two or more correlated receiver operating characteristic curves: a nonparametric approach. *Biometrics*. 1988;44:837–845.
19. Lee SY, Lee EK, Park KH, Kim DM, Jeoung JW. Asymmetry analysis of macular inner retinal layers for glaucoma diagnosis: swept-source optical coherence tomography study. *PLoS One*. 2016;11:e0164866.
20. Hirasawa H, Araie M, Tomidokoro A, et al. Reproducibility of thickness measurements of macular inner retinal layers using SD-OCT with or without correction of ocular rotation. *Invest Ophthalmol Vis Sci*. 2013;54:2562–2570.
21. Chauhan BC, Sharpe GP, Hutchison DM. Imaging of the temporal raphe with optical coherence tomography. *Ophthalmology*. 2014;121:2287–2288.
22. Mori S, Kurimoto T, Kanamori A, et al. Discordance of disc-fovea raphe angles determined by optical coherence tomography and MP-3 microperimetry in eyes with a glaucomatous hemifield defect. *Invest Ophthalmol Vis Sci*. 2019;60:1403–1411.